Original Article

RAMP1 Protects Hepatocytes against Ischemia-reperfusion Injury by Inhibiting the ERK/YAP Pathway

Yongsheng Tang[1#], Zenan Yuan[1#], Xu Lu[1], Yingqiu Song[2], Shuguang Zhu[1], Chunhui Qiu[1], Qi zhang[3], Binsheng Fu[1], Changchang Jia[3*] and Hua Li[1]

[1]Department of Hepatic Surgery, Liver Transplantation Center, The Third Affiliated Hospital of Sun Yat-sen University, Guangzhou, Guangdong, China; [2]Department of Gastrointestinal Surgery, The Third Affiliated Hospital of Sun Yat-sen University, Guangzhou, Guangdong, China; [3]Department of Cell-Gene Therapy Translational Medicine Research Center, The Third Affiliated Hospital of Sun Yat-sen University, Guangzhou, Guangdong, China

Abstract

Background and Aims: Hepatic ischemia-reperfusion injury (HIRI) is a prevalent complication of liver transplantation, partial hepatectomy, and severe infection, necessitating the development of more effective clinical strategies. Receptor activity–modifying protein 1 (RAMP1), a member of the G protein–coupled receptor adapter family, has been implicated in numerous physiological and pathological processes. The study aimed to investigate the pathogenesis of RAMP1 in HIRI. ***Methods:*** We established a 70% liver ischemia-reperfusion model in RAMP1 knockout (KO) and wild-type mice. Liver and blood samples were collected after 0, 6, and 24 h of hypoxia/reperfusion. Liver histological and serological analyses were performed to evaluate liver damage. We also conducted in-vitro and in-vivo experiments to explore the molecular mechanism underlying RAMP1 function. ***Results:*** Liver injury was exacerbated in RAMP1-KO mice compared with the sham group, as evidenced by increased cell death and elevated serum transaminase and inflammation levels. HIRI was promoted in RAMP1-KO mice via the induction of hepatocyte apoptosis and inhibition of proliferation. The absence of RAMP1 led to increased activation of the extracellular signal–regulated kinase (ERK)/mitogen-activated protein kinase (MAPK) pathway and yes-associated protein (YAP) phosphorylation, ultimately promoting apoptosis. SCH772984, an ERK/MAPK phosphorylation inhibitor, and PY-60, a YAP phosphorylation inhibitor, reduced apoptosis in *in-vitro* and *in-vivo* experiments. ***Conclusions:*** Our findings suggest that RAMP1 protects against HIRI by inhibiting ERK and YAP phosphorylation signal transduction, highlighting its potential as a therapeutic target for HIRI and providing a new avenue for intervention.

Introduction

Hepatic ischemia-reperfusion injury (HIRI) is a major form of liver damage that can occur during surgeries, such as partial hepatectomy and liver transplantation,[1] and with conditions such as hemorrhagic shock and severe infection.[2] It has two stages: initial cellular damage due to hypoxia and the subsequent restoration of oxygen delivery, and subsequent toxic effects of oxygen reperfusion on ischemic tissue. These effects can further exacerbate liver dysfunction and damage, leading to processes such as inflammatory cell infiltration, the production and release of cytokines and chemokines, oxygen-free radical production and destruction, and mitochondrial Ca^{2+} overload.[3–7] Despite extensive research on HIRI, effective drugs for clinical use are lacking, and the identification of viable drug targets is critical for the development of clinical therapies. G protein–coupled receptors (GPCRs) form the largest class of cell surface receptors in humans and a major drug target category. Our research focuses on the identification of GPCRs associated with HIRI, with the aim of discovering new therapeutic targets to guide effective drug development and provide novel approaches to the clinical treatment of HIRI.

We are particularly interested in GPCRs that have been shown to regulate inflammation and injury repair, such as

calcitonin gene–related peptide (CGRP) receptors. Receptor activity-modifying protein 1 (RAMP1) and calcitonin-like receptor (CLR) are the two main components of these receptors, involved in processes such as vasodilation, pain stimulation, and inflammation.[8] RAMP1 has been studied extensively due to its ability to reduce inflammation,[9,10] and promote injury repair.[11,12] As the alteration of its expression can modulate the sensitivity of CGRP, and as it binds to and regulates CLR expression, the targeting of RAMP1 may be a promising approach to the alteration of CGRP activity.[13] RAMP1-deficient mice exhibit impaired organ mass recovery and hepatocyte proliferation, which stimulates the expression and activity of yes-associated protein (YAP)/TAZ after 70% hepatectomy or repeated intraperitoneal injection of carbon tetrachloride.[14] Additionally, RAMP1 is involved in the regulation of apoptosis, and the in-vitro and in-vivo inhibition of the CGRP/CRLR + RAMP1 signaling pathway can induce apoptosis in EVI1-high AML cells by disrupting extracellular signal–regulated kinase (ERK)/mitogen-activated protein kinase (MAPK) signaling.[15] The ERK/MAPK pathway is known to be involved in the regulation of various cellular processes, including cell proliferation, differentiation, and apoptosis.[16] The excessive activation and increased expression of ERK1/2 may promote apoptosis and worsen IRI.[17–19] The investigation of whether the expression of RAMP1 is altered during HIRI and whether RAMP1 affects apoptosis through the ERK/MAPK pathway is crucial. Whether RAMP1 deficiency affects YAP phosphorylation in this context is also worth exploring. Thus, we investigated the role of ERK1/2 in HIRI.

This study revealed that RAMP1 expression is significantly increased in the livers of mice treated with liver I/R, suggesting that RAMP1 plays a role in this process. Our in-vivo and in-vitro experiments showed that RAMP1 alleviates liver injury by reducing hepatocyte apoptosis and the inflammatory response via the ERK/MAPK pathway. Moreover, we found that RAMP1 decreases YAP phosphorylation, thereby promoting hepatocyte activity. Our findings suggest that RAMP1 serves as a pivotal regulator in HIRI and is a promising target for clinical intervention.

Methods

Animals

Male RAMP1 knockout (RAMP1-KO) mice aged 6–8 weeks were obtained from Jiangsu Gempharmatech Biological Science and Technology Ltd (Nanjing, Jiangsu, China) and bred at the Guangzhou Ruiye Animal Model Center. CRISPR-Cas9 technology was used to edit RAMP1 in the KO mice. All mice were maintained on a 12/12-hour light/dark cycle and provided with food and water.

Hepatic ischemia-reperfusion injury mouse models

A non-lethal segmental (70%) hepatic warm ischemia-reperfusion model was established in both WT and RAMP1-KO mice.[20] Microvascular clamps were used to block the first porta hepatis for 90 min, followed by reperfusion. Mice were sacrificed at 0, 6, and 24 h after reperfusion, and liver and blood samples were collected. The sham group underwent identical procedures but without the hepatic portal vein being blocked.

Immunohistological and the terminal deoxynucleotidyl transferase-mediated dUTP-digoxigenin nick end labeling (TUNEL) staining

Immunohistological staining of liver samples was performed according to the manufacturer's protocol. Briefly, following a sequence of fresh xylene, 100 % ethanol, 100 % ethanol,

95 % ethanol, and 75 % ethanol passing through the cylinder, along with EDTA antigen repair, the slides were then incubated with RAMP1 antigen antibodies (ab203282, abcam) and Ki67 antibodies (ab15580, abcam). Subsequently, the sections were stained with Dako secondary antibody (DAKO immunohistochemical kit REAL EnVision) and counterstained with hematoxylin. Hematoxylin and eosin (H&E) staining were used to observe pathological changes in the liver ischemia-reperfusion area of the mice. The TUNEL assay was performed using an in situ cell death detection kit (11684817910, Roche).[21] Nuclei were stained with DAPI (62248, ThermoFisher Scientific). Nuclei with clear red staining indicated TUNEL-positive apoptotic cells. The mean ± standard deviation (SD) of positive cells per 1,000 samples was calculated, followed by counting the labeled cells in 10 fields of view at 200× magnification.

Liver function assay and histologic examination

Serum alanine aminotransferase (ALT) and aspartate aminotransferase (AST) levels were measured as indicators of liver injury using an automatic analyzer (Antech Diagnostics, Los Angeles, California, USA). Paraffin-embedded formalin-fixed liver tissue was cut into 4-μm thick sections. The sections were stained with (H&E),[22] and inflammation and tissue damage were blindly analyzed using Suzuki's standard.[23]

Primary hepatocyte isolation

As described previously,[21,22,24] primary hepatocytes were isolated from mice aged 6–8 weeks. Briefly, after anaesthesia, the mice were infused with a buffer solution (lacking Ca^{2+} and Mg^{2+}) through the portal vein. Liver perfusion was performed using 0.05% type IV collagenase (C5138, Sigma), followed by resection and filtration through a 0.22-μm cell filter (SLGP033RB, Millipore). Hepatocytes were isolated and collected in DMEM (C11995, GIBCO).

Cell culture and hepatocyte hypoxia/reoxygenation (H/R) model

Primary hepatocytes or L02 cells were cultured in DMEM/F12 containing 10% fetal bovine serum (FBS) in a humidified atmosphere of 5% CO_2 at 37°C. The I/R model was simulated *in vitro* and the cells were treated with H/R. Primary hepatocytes initially placed in glucose-free DMEM (C11995, GIBCO) were cultured under hypoxic conditions (1% oxygen) for 4 h, followed by exposure to normoxic conditions.[21]

Western blot analysis

Total protein was extracted from the liver tissue and primary hepatocytes following the manufacturer's protocol. The samples were then separated on 12% sodium dodecyl sulfate-polyacrylamide gels (Bio-Rad, Hercules, CA, USA) and transferred onto polyvinylidene fluoride membranes (Millipore, Bedford, MA, USA). The membranes were blocked with 5% skim milk powder at 25°C for 1 h and incubated overnight at 4°C with the following primary antibodies targeting the following proteins: RAMP1(ab156575, abcam), Bcl-2 (Cat. #3498S, Cell Signaling Technology [CST]), Bax (Cat. #2772S, CST), Caspase-3 (Cat. #9662S, CST), ERK1/2 (Cat. #9102S, CST), p-ERK1/2 (Cat. #9101S, CST), JNK (Cat. #9252S, CST), p-JNK (Cat. #4668S, CST), P38 (Cat. #8690S, CST), p-P38 (Cat. #4511S, CST), YAP (Cat. #14074S, CST), p-YAP (Cat. #4911S, CST), β-actin (Cat. #4967S, CST).

Quantitative real-time polymerase chain reaction (qRT-PCR)

Total RNA was isolated using TRIzol (15596026, ThermoFish-

er), while cDNA synthesis was carried out using the Hiscript III RT Supermix for QPCR (+gDNA Wiper) kit, following the manufacturer's instructions. Subsequently, the cDNA was quantified using a LightCycler 480 high-throughput real-time fluorescent quantitative PCR instrument. The mRNA expression level was normalized to 18s rRNA level. Primers for qRT-PCR were synthesized by Tsingke Company in Wuhan.

Cell Counting Kit-8 assay (CCK-8)

Adherent primary hepatocytes were plated in 96-well plates, and each group was spread with 3–5 holes. Each hole was filled with 200 µL medium or configured drugs. During the detection, the culture medium was replaced, 10 µL CCK-8 (KGA317-2, KeyGEN) and 100µL culture medium (C11875500BT, GIBCO) were added to each well, and incubated at 37°C for 2 h. Finally, the absorbance at 450 nm was measured using a microplate reader.

Drug

YAP phosphorylation inhibitor: Truli[25] (E1061, Selleck, 0.2 nm) and PY-60[26] (HY-141644, MCE; 1.6 µm; 10 mg/kg for mice *in vivo*, *i.p.*); ERK phosphorylation inhibitor: Temuterkib[27] (HY-101494, MCE; 5 nm) and SCH772984[28] (HY-50846, MCE; 300 nm, 5 mg/kg for mice *in vivo*, *i.p.*[29]); ERK agonist: C16-PAF(HY-108635, MCE, 1 µm[30,31]); STAT3 inhibitor : Sttatic[32] (HY-13818, MCE; IC50:10 µm); p-AKT inhibitor: MK2206[33] (HY-10358, MCE; 65 nm); Caspase-3 inhibitor: Z-VAD (HY-16658B, MCE; 10 µm[34]; 10 mg/kg for mice *in vivo*, *i.p.*[35]); CGRP agonist: Calcitonin Gene Related Peptide (CGRP) II, rat TFA (HY-P1913A , MCE; 83 µm[36]); Verteporfin (HY-B0146, MCE; 5 µm[37]).

Caspase-3 activity assay

Caspase-3 activity assays were conducted using the Caspase-3 Activity Assay Kit (C1115, Beyotime), following previously established protocols.[38,39] Briefly, liver tissue treated with pyrrolidine lysate was lysed using lysis buffer. The supernatants obtained from the homogenates were collected by centrifugation at 16,000 g for 15 min, and the protein concentration was quantified using the Bradford Protein Assay kit (P0006, Beyotime). Subsequently, the lysates were incubated with Ac-DEVD-pNA (2 mmol/L) at 37°C for 2 h. After incubation, the absorbance was measured at 405 nm using a microplate reader (BioTek).

Caspase-3 Activity and Apoptosis Detection Kit for Live Cell (C1077M, Beyotime)

Following H/R, the cell culture medium was aspirated into a suitable centrifuge tube and the cells were rinsed once with PBS. An appropriate volume of trypsin cell digestion solution was added for cell detachment. The cells were collected, transferred to a centrifuge tube, and centrifuged at 2,000 rpm for 5 min, The supernatant was discarded, and the cells were gently suspended in PBS. The resuspended cells were centrifuged at 2,000 rpm for 5 min, and the supernatant was discarded. In total, 194µL Annexin V-mCherry Binding Buffer was added to gently resuspend the cells. Furthermore, 5 µL Annexin V-mCherry and 1µL GreenNuc™ Caspase-3 Substrate (1 mM) were added and mixed gently. The mixture was incubated at room temperature (20–25°C) for 20–30 min in the dark. GreenNuc™-DNA exhibited green fluorescence (excitation/emission=500/530 nm), whereas Annexin V-mCherry displayed red fluorescence (excitation/emission=587/610 nm). Cells were collected and gently suspended in 100 µL Annexin V-mCherry Binding Buffer. After smearing, the cells were observed using an Elyra 7 Lattice SIM (Zeiss, Germany). We followed identical procedures for flow cytometry experiments, employing Gallios (Beckman Coulter) flow cytometers for the analyses, and the data were analyzed using CytExpert software packages.

Flow cytometric analysis of apoptotic cell

Cells were collected as described previously. The supernatant was discarded and 2 µL Propidium iodide (PI) and 2 µL Annexin V (KGA107, KeyGEN) were added and mixed gently. Cells were suspended with 250 µL Binding Buffer and incubated at room temperature (20–25°C) for 20–30 min in the dark. Flow cytometric analyses were performed using a Gallios flow cytometer (Beckman Coulter), and the data were analyzed using the CytExpert software package.

Immunofluorescence staining

To analyze immune cell accumulation in the liver, immunofluorescence staining of monocytes was performed using primary antibodies against mouse CD68 (ab125212; abcam) and RAMP1 (ab203282; abcam). Goat anti-rabbit and anti-mouse IgG (Invitrogen) were used as the secondary antibodies. A 488 nm wavelength laser was employed to excite the fluorescein tag (green emission for imaging), and a 555 nm wavelength laser was used for the fluorescein tag (red emission for imaging) (G1236-100T, Servicebio). DAPI was excited using UV light (blue emission for imaging). The images were obtained using three emerging channels. GreenNuc™-DNA and Annexin V-mCherry (C1077M, Beyotime) were used to monitor Caspase-3 activity and apoptosis in living cells, and images were generated from both channels. The co-localization of RAMP1 and macrophages was detected using confocal microscopy (LSM980, Zeiss, Germany).

Transmission electron microscopy

The anaesthetized mice were perfused with 0.9% saline, and 1 mm^3 liver tissue blocks were obtained. Next, the fresh tissue blocks were immersed in fixative for transmission electron microscopy (Servicebio) at 4°C for 4 h. They were then treated with 1% OsO4 in 0.1 mol/L PBS for 2 h at room temperature, followed by a dehydration process with gradient alcohol. Subsequently, the sections were embedded and underwent baking in an oven at 60°C for 48 h and were cut into ultrathin sections (60 nm) using an ultramicrotome. Finally, the ultrastructure of the tight junctions of the liver was observed using a transmission electron microscope (HITACHI, HT7700) as described previously.[40]

Statistical analyses

Data were expressed as the means ± SDs, including IHC staining and western blot results. Statistical differences between the two groups were analyzed using a two-tailed unpaired Student's t-test. $p < 0.05$ was considered statistically significant by GraphPad Prism 8.0.1 (GraphPad Software, USA).

Results

RAMP1 upregulation was related closely to HIRI

To examine the changes in RAMP1 in HIRI, we created an in-vivo model of HIRI in mice and an in-vitro model of hypoxia/reoxygenation (H/R) treatment of primary hepatocytes isolated from mice. RAMP1 expression was upregulated at the protein and mRNA levels in the HIRI model and peaked at 6 h after I/R treatment (Fig. 1A–C). Primary hepatocytes from wild-type (WT) mice treated with H/R also showed increases in RAMP1 protein levels compared with control hepatocytes
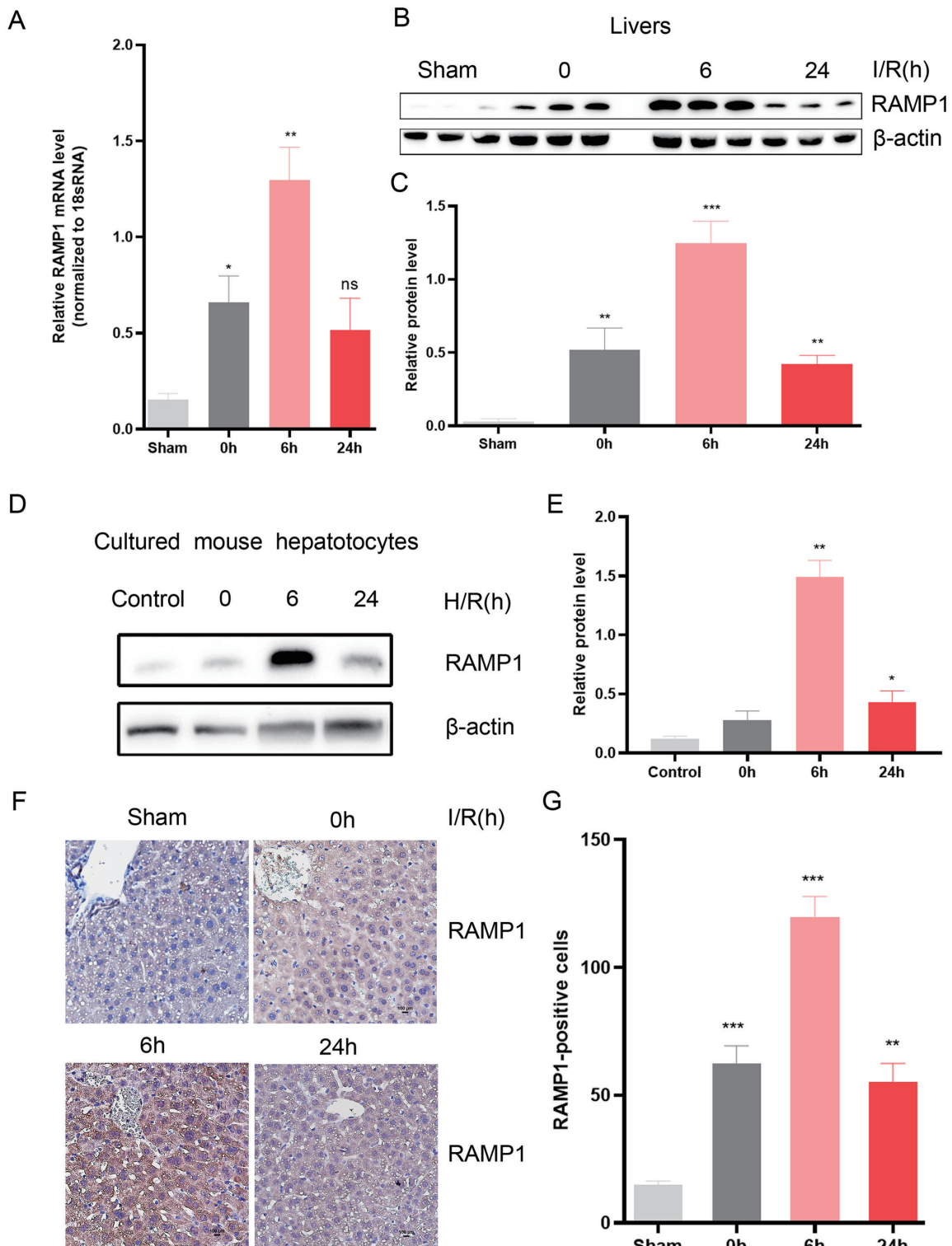
Fig. 1. Change of RAMP1 expression in HIRI. (A) mRNA and (B) RAMP1 protein levels in liver tissues from mice subjected to sham treatment (sham) or 90 min of ischemia followed by reperfusion (I/R) for the indicated times (n=3–5 per time point). (C) Quantitative expression of RAMP1 protein of mouse livers. (D) Western blot analysis to measure RAMP1 protein levels in primary hepatocytes exposed to either a control treatment (control) or hypoxia for 90 min followed by reoxygenation (H/R), across designated time periods. (F) Immunohistochemical staining and (G) quantitative expression of RAMP1 in liver tissues subjected to control treatment or hypoxia for 90 min followed by reoxygenation, across designated time periods. For B and D, β-actin served as the loading control in western blot. For A, 18s rRNA served as the loading control in quantitative RT-PCR. All data are presented as the mean ± SD; *p<0.05, **p<0.01, ***p<0.001 compared with the sham or control group using Student's two-tailed t-test. RAMP1, receptor activity–modifying protein 1; I/R, ischemia/reperfusion; H/R, hypoxia/reoxygenation; HIRI, hepatic ischemia-reperfusion injury.

(Fig. 1D, E). Immunohistochemical analysis confirmed that RAMP1 expression peaked at 6 h after I/R treatment (Fig. 1F, G).

RAMP1 ameliorates liver damage induced by HIRI

To investigate the role of RAMP1 in HIRI *in vivo*, we generated RAMP1- knockout (KO) mice. The mice exhibited RAMP1 deficiency in the liver (Fig. 2A) and hepatocytes (Fig. 2B), and showed no signs of liver damage under sham conditions (Fig. 2C). Following the HIR operation, RAMP1-KO and WT mice had increased serum ALT and AST levels reflecting liver damage, which were higher in the former group (Fig. 2C, D). Histological analysis of liver tissue obtained immediately after reperfusion showed normal hepatocyte morphology and lobular structure in the sham group, and mild to moderate hepatocyte swelling and mild hepatic sinus dilation in the WT and RAMP1-KO groups. At 6 h after reperfusion, severe hepatocyte swelling, inflammatory cell infiltration, and patchy necrosis were observed in the RAMP1-KO and WT groups, and were more serious and extensive in the former (Fig. 2E, F). Consistent with these histological assessments, the necrotic area and Suzuki score were significantly elevated in the RAMP1-KO group compared with those in the WT group (Fig. 2G). Levels of the inflammatory factors IL-6, IL-1β, and TNF-α, detected by quantitative RT-PCR (Supplementary Table 1), showed similar changes over time in both groups (Supplementary Fig. 1A, C, D). However, the level of the protective inflammatory factor IL-10 was significantly decreased in the RAMP1-KO group at 6 h after reperfusion (Supplementary Fig. 1B). These findings suggest that RAMP1 plays a protective role against HIRI in mice.

RAMP1 inhibited hepatocyte apoptosis and promoted liver proliferation in HIRI

As apoptosis is the primary manifestation of HIRI, we determined the apoptotic rate in liver tissues using TUNEL staining. We found that RAMP1 deficiency worsened apoptosis, especially at 6 h after I/R (Fig. 3A, B). Under sham conditions, TUNEL signals were undetectable in WT and RAMP1-KO mouse livers. Relative to those of WT mice, the livers of RAMP1-KO mice showed reduced expression of Bcl-2 (a pro-survival gene) and increased expression of Bax (a pro-apoptotic gene) (Fig. 3C, Supplementary Fig. 2A). Western blot analysis revealed that HIRI induced greater expression of cleaved Caspase-3 in the RAMP1-KO group than in the WT group (Fig. 3C, Supplementary Fig. 2B). The same phenomenon was observed in primary hepatocytes (Fig. 3D, Supplementary Fig. 2C, D). Transmission electron microscopy also showed distinct indications of apoptosis (Supplementary Fig. 3A, B).

Conversely, significantly fewer Ki67-positive cells were observed in the RAMP1-KO group than in the WT group (Fig. 3E, F). We examined alterations in Caspase-3 activity during HIRI and used Annexin V staining to detect apoptosis (Fig. 4A, B). The red and green fluorescence of hepatocytes increased notably during hepatic I/R and weakened upon treatment with Z-VAD (a Caspase-3 inhibitor). Flow cytometry demonstrated significant increases in apoptosis and Caspase-3 activity during H/R and a decrease in the proportion of apoptotic cells upon Caspase-3 activity inhibition (Fig. 4C–F). Similarly, Z-VAD tended to reduce liver cell injury in the I/R animal model (Fig. 4G–J, Supplementary Fig. 3C). The cell and animal experiments consistently showed increases in hepatocyte apoptosis and Caspase-3 activity during HIRI. The results suggest that RAMP1 inhibits hepatocyte apoptosis and promotes liver proliferation during HIRI.

RAMP1 protects hepatocytes against IRI by inhibiting the ERK/MAPK pathway and YAP phosphorylation

At 6 h after HIR, the number of cleaved Caspase-3–positive cells peaked and the phosphorylation of YAP was significantly enhanced, suggesting that apoptosis was the most severe. To identify the pathway that was significantly activated to cause increased apoptosis after RAMP1-KO, we used YAP and ERK phosphorylation inhibitors. CCK-8 revealed no significant effect on the activity of WT or RAMP1-KO primary hepatocytes under normoxic conditions (Fig. 5A). Under H/R, the YAP phosphorylation inhibitor PY-60 and ERK phosphorylation inhibitor SCH772984 significantly inhibited the H/R-induced apoptosis of RAMP1-KO primary hepatocytes (Fig. 5B). Other pathways, such as those of p-AKT and STAT3, did not significantly alter cell activity after inhibitor use under H/R. We detected changes in the MAPK pathway in WT and RAMP1-KO primary hepatocytes after H/R treatment. RAMP1-KO primary hepatocytes did not affect basic JNK, ERK1/2, or p38 signal transduction under control conditions (Fig. 5C–F). After 6 h of H/R treatment, the phosphorylation of JNK showed no significant change, that of p38 was significantly decreased, and that of ERK1/2 was significantly increased compared with those in the WT group. The phosphorylation of YAP is also shown in Figure 5C and G. Similar results were observed in WT and RAMP1-KO mice after HIRI, suggesting that RAMP1 affects apoptosis through ERK/MAPK and YAP (Fig. 5H–L).

RAMP1 protects hepatocytes against IRI by inhibiting the ERK/YAP pathway

The detection of apoptosis-related protein levels in primary hepatocytes after 6 h of H/R using the YAP phosphorylation inhibitor PY-60 and the ERK1/2 phosphorylation inhibitor SCH772984 showed different degrees of increased Bcl-2 expression and reduced Bax and cleaved Caspase-3 expression (Fig. 6A–C). These effects were also observed in the livers of RAMP1-KO mice (Fig. 6D–F). In the animal model, PY-60 and SCH772984 significantly reduced HIRI, protecting hepatocytes (Supplementary Fig. 4A–E). These results indicate that RAMP1 regulates HIRI-related apoptosis through ERK/MAPK and YAP.

Primary hepatocytes subjected to hypoxia and treated with PY-60 for 6 h showed reduced YAP phosphorylation, suggesting YAP pathway inhibition. However, the phosphorylation of ERK1/2 did not change; with SCH772984 administration during the sixth hour of H/R, the p-ERK1/2 level decreased as expected and YAP phosphorylation decreased significantly relative to the control (Fig. 6G). To elucidate the regulatory interplay among RAMP1, ERK1/2, and YAP, we employed the CGRP agonist CGRP II, rat TFA, known to efficaciously activate RAMP1 (Fig. 7A, B). Subsequently, CGRP agonists, an ERK inhibitor and agonist, and a YAP inhibitor and agonist were employed in the H/R model for CCK-8 analysis. CGRP agonist treatment substantially reduced H/R damage and increased cell activity, whereas the co-administration of a CGRP agonist with an ERK agonist (C16-PAF) or YAP inhibitor (verteporfin) significantly reduced cell activity. The co-administration of the CGRP agonist with SCH772984 or PY-60 increased cell activity (Fig. 7C, D), implying that RAMP1 acts upstream of YAP and ERK1/2. We administered SCH772984 with Verteporfin or PY-60 to scrutinize the regulatory relationship between ERK1/2 and YAP. SCH772984 and SCH772984 + PY-60 significantly boosted cell activity during H/R, whereas SCH772984 + Verteporfin notably reduced this activity. Conversely, C16-PAF + Verteporfin markedly reduced
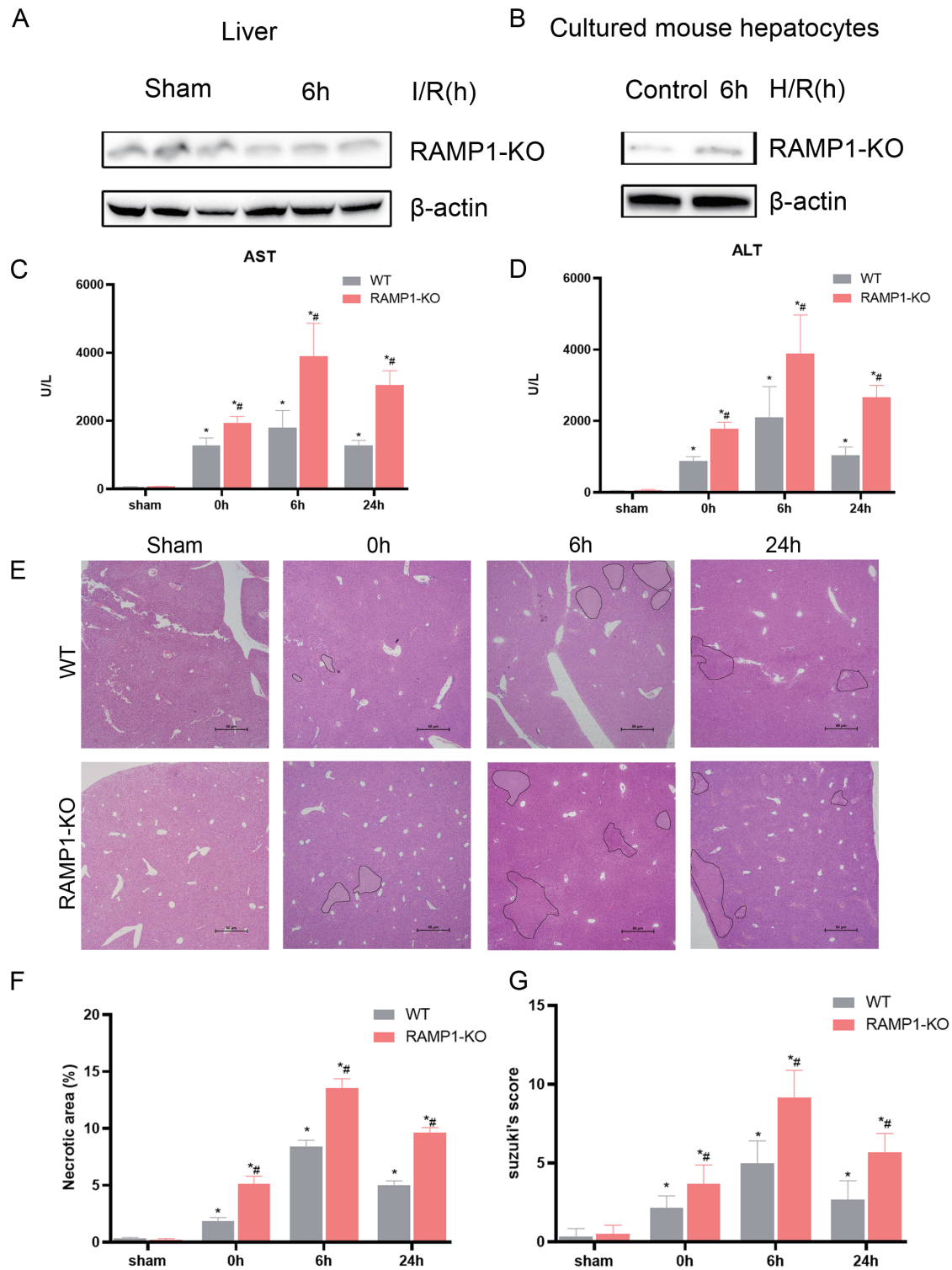
Fig. 2. Effect of RAMP1 upregulation in HIRI. (A) Western blot analysis was conducted to evaluate RAMP1 expression in liver tissues and primary hepatocytes (B) derived from RAMP1-KO mice (n=3–5 per time point). (C) The levels of serum AST and (D) ALT were measured in WT or RAMP1-KO mice that were subjected to either a sham procedure or hepatic I/R at various time points, as indicated. (n=3–5 per time point). (E) The necrotic areas in the livers of WT and RAMP1-KO mice were evaluated using representative histological H&E staining images and statistical analysis (F) after hepatic I/R operations at different time points, as indicated (n=3–5 per group). (G) Suzuki's scores of liver sections (n=3–5 per group) were also determined. β-actin served as the loading control. The circle sign indicates the necrotic area. All data are presented as the mean ± SD. *$p<0.05$ compared with the sham groups; #$p<0.05$ compared with the WT+I/R groups using Student's two-tailed t-test. RAMP1-KO, RAMP1 knockout; ALT, alanine aminotransferase; AST, aspartate aminotransferase; I/R, ischemia/reperfusion; H&E, hematoxylin and eosin; HIRI, hepatic ischemia-reperfusion injury; WT, wild-type.
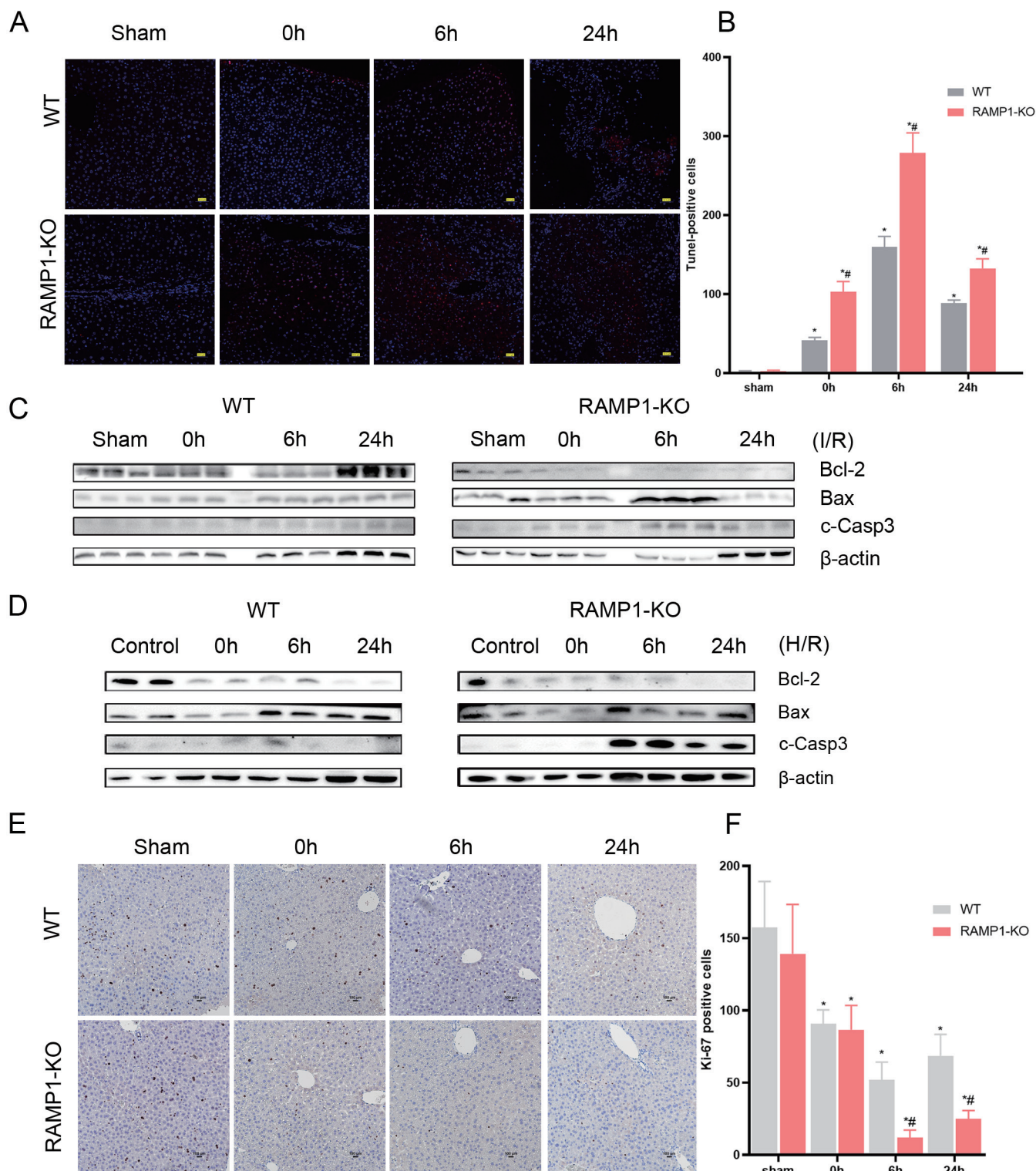
Fig. 3. Effect of RAMP1 on apoptosis and proliferation *in vitro* and *in vivo*. (A) Representative images and (B) statistical analysis of TUNEL assays were performed on liver lobes obtained from WT and RAMP1-KO mice after hepatic I/R at different time points, as indicated (n=3–5 per group). (C) Protein levels of pro-apoptotic or pro-survival genes in the livers of WT and RAMP1-KO mice that underwent hepatic I/R operations (n=3–5 per group). (D) Protein levels of pro-apoptotic or pro-survival genes in primary hepatocytes of WT and RAMP1-KO mice that underwent H/R treatment (n=3–5 per group). (E) (F) Histological staining images and statistical analysis of Ki67 expression in liver tissues. β-actin served as the loading control. All data are presented as the mean ± SD. *$p<0.05$ compared with the sham groups; #$p<0.05$ compared with the WT + I/R groups using Student's two-tailed t-test. c-Casp-3, cleaved-Caspase3; Bax, bcl2-associated X protein; Bcl2, b-cell leukemia/lymphoma; HIRI, hepatic ischemia-reperfusion injury; TUNEL, terminal deoxynucleotidyl transferase deoxyuridine triphosphate nick end-labeling.
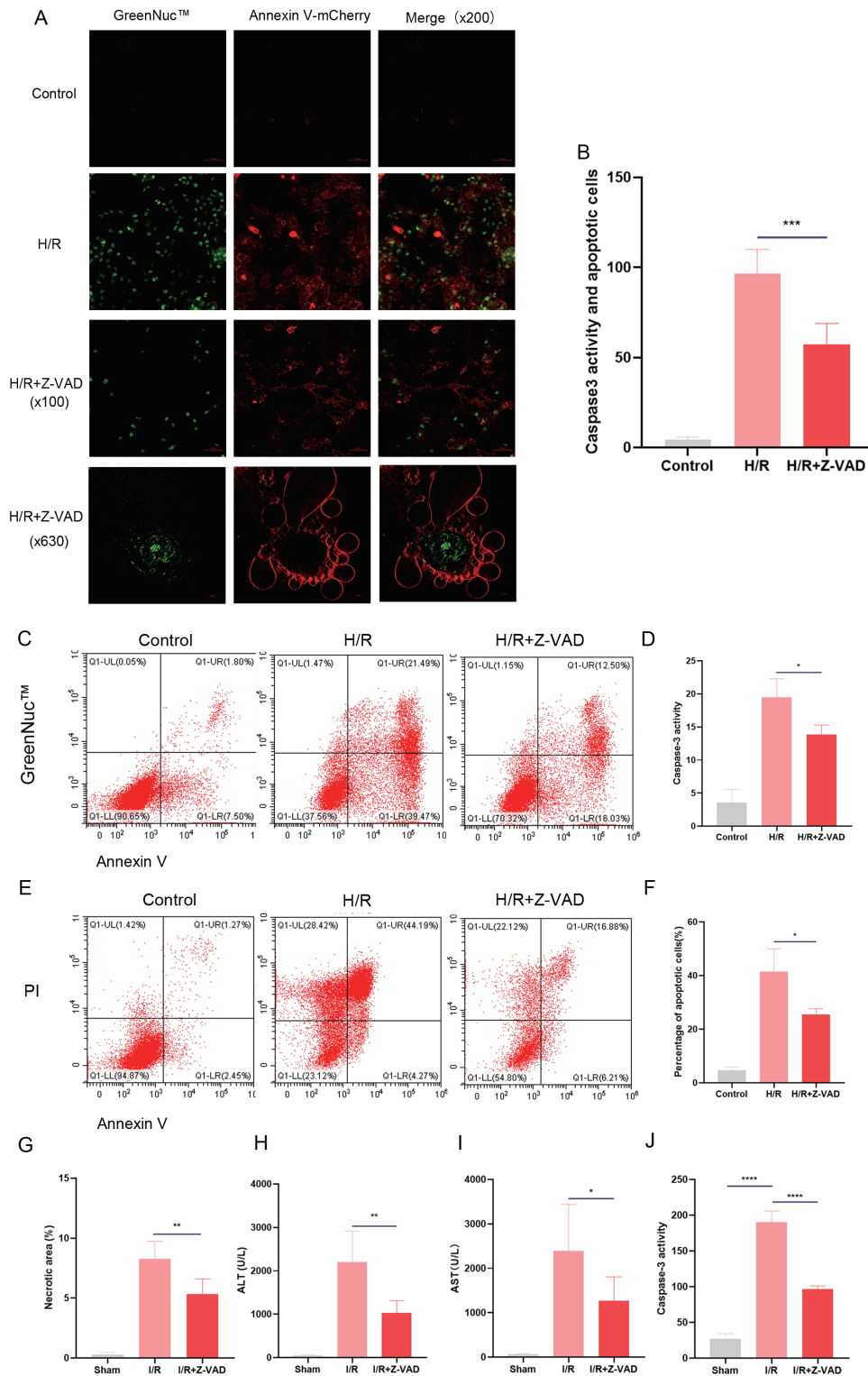
Fig. 4. Change of Caspase-3 activity and occurrence of apoptosis during HIRI. (A) Live cell Caspase-3 activity and apoptosis detection kit were used to detect Caspase-3 activity and apoptosis in L02 cells (human hepatocytes) via fluorescence microscopy after using Z-VAD (Caspase-3 inhibitor) in Control and H/R. (B) Statistical analysis of A. (C) Live cell Caspase-3 activity and apoptosis detection kit was used to detect Caspase-3 activity and apoptosis in L02 cells via flow cytometry after using Z-VAD in Control and H/R. (D) Statistical analysis of C. (E) Annexin V-FITC/PI apoptosis detection kit was used to detect apoptosis in L02 cells after using Z-VAD under Control and H/R. (F) Statistical analysis of E. (G) Statistical analysis of HE staining necrosis area of liver in sham and I/R mice using Z-VAD. (H) ALT. (I) AST. (J) Caspase-3 activity was measured by spectrophotometry. All data are presented as the mean ± SD. *p<0.05, **p<0.01,***p<0.001, ****p<0.0001 using Student's two-tailed t-test. ALT, alanine aminotransferase; AST, aspartate aminotransferase; H/R, hypoxia/reoxygenation; HIRI, hepatic ischemia-reperfusion injury.
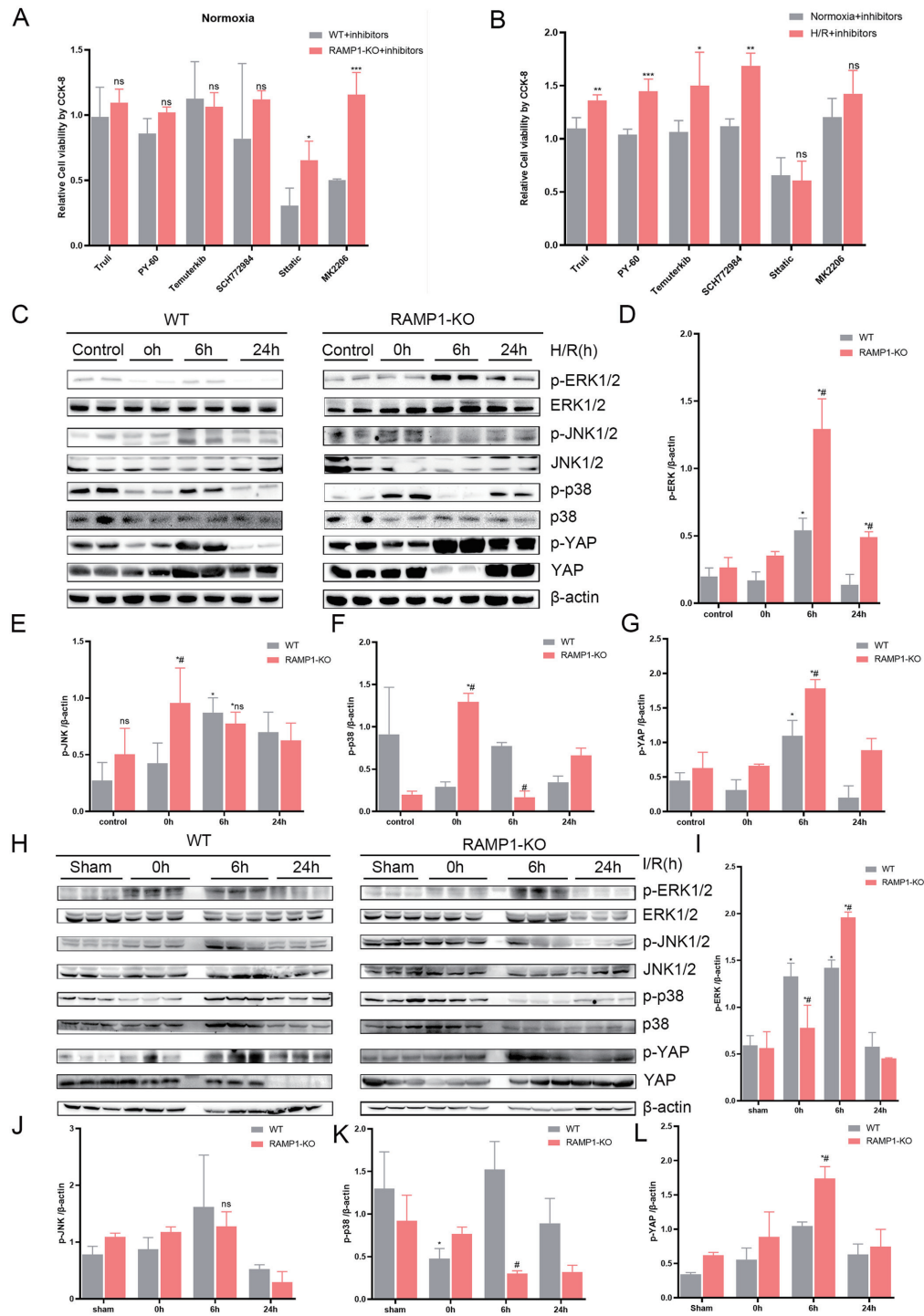
**Fig. 5. Effect of RAMP1 on ERK/MAPK pathway and YAP phosphorylation in HIRI.** (A) The CCK-8 assay was conducted on primary hepatocytes from WT mouse livers that were treated with inhibitors associated with apoptosis pathways, both under normoxia and after 6 h. (B) A CCK-8 assay was conducted on primary hepatocytes from RAMP1-KO mouse livers treated with inhibitors associated with apoptosis pathways, both in normoxia and after 6 h of H/R treatment. Western blot analysis was performed to detect the activation of MAPK signaling pathways and YAP phosphorylation in primary hepatocytes (C) and livers (H) from these mice, and statistical analysis was conducted for primary hepatocytes (D-G) and livers (I-L) (n=3–5 per group). All data are presented as the mean ± SD. For A, *$p<0.05$, **$p<0.01$, ***$p<0.001$ compared with the WT group with the same treatment using Student's two-tailed t-test. B, *$p<0.05$, **$p<0.01$, ***$p<0.001$ compared with the groups under normoxia with the same treatment using Student's two-tailed t-test; D and F, *$p<0.05$, compared with the sham/control groups; #$p<0.05$ compared with the WT I/R groups using Student's two-tailed t-test. Truli and PY-60: YAP phosphorylation inhibitors, Temuterkib and SCH772984: ERK phosphorylation inhibitors, Stattic: STAT3 inhibitor, and MK2206: P-AKT inhibitor. CCK-8,cell counting Kit-8; CGRP,caltonin gene-related peptide; ERK1/2, extracellular signal–regulated kinase1/2; HIRI, hepatic ischemia-reperfusion injury; JNK1/2, c-Jun NH2-terminal kinase1/2; MAPK, mitogen-activated protein kinase; p-ERK1/2, phosphorated extracellular signal–regulated kinase1/2; p-JNK1/2, phosphorated c-Jun NH2-terminal kinase1/2; p-YAP, phosphorated yes-associated protein; STAT3, signal transducer and activator of transcription 3; VP, verteporfin; WT, wild-type; YAP, yes-associated protein.
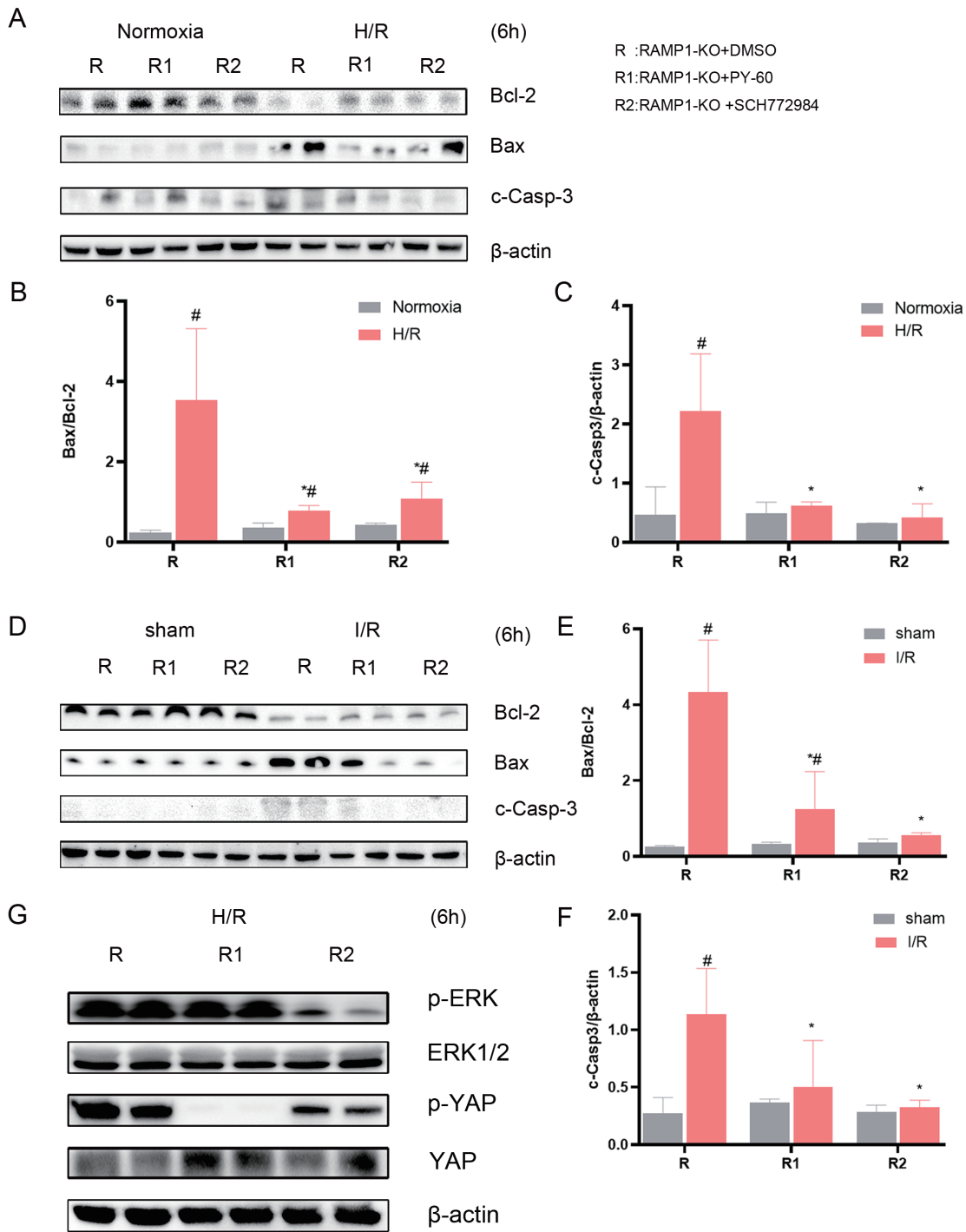
Fig. 6. Effect of changing ERK and YAP on apoptosis during HIRI. (A) Protein levels, (B) and (C) statistical analysis of pro-apoptotic and anti-apoptotic genes in primary hepatocytes from RAMP1-KO mice. The cells were treated with apoptosis pathway inhibitors and subjected to 6 h of reperfusion after hypoxia. (D) Protein levels, (E) and (F) statistical analysis of pro-apoptotic and anti-apoptotic genes measured in liver tissues from RAMP1 KO mice subjected to hepatic ischemia-reperfusion (I/R) surgery. Mice were treated with apoptosis pathway inhibitors and subjected to 6 h of reperfusion. (G) The protein levels of YAP and ERK1/2 and their respective phosphorylation states were assessed in primary hepatocytes isolated from RAMP1-KO (RAMP1 knockout) mice. The hepatocytes were then treated with inhibitors targeting this pathway and subsequently subjected to a 6 h reperfusion period following a period of hypoxia. All data are presented as the mean ± SD. B, *$p<0.05$, compared with the R group; #$p<0.05$ compared with the groups in normoxia with the same treatment using Student's two-tailed t-test. D, *$p<0.05$, compared to the R group; #$p<0.05$ compared to the groups in sham with the same treatment using Student's two-tailed t-test. R group: primary hepatocytes or liver from RAMP1-KO mice + DMSO; R1 group: primary hepatocytes or liver from RAMP1-KO mice + PY-60; R2 group: primary hepatocytes or liver from RAMP1-KO mice + SCH772984. I/R, ischemia/reperfusion; H/R, hypoxia/reoxygenation; ERK1/2, extracellular signal–regulated kinase; p-ERK1/2, phosphorated extracellular signal–regulated kinase; YAP, yes-associated protein; p-YAP, phosphorated yes-associated protein; c-Casp-3, cleaved-Caspase3; Bax, bcl2-associated X protein; Bcl2, b-cell leukemia/lymphoma; HIRI, hepatic ischemia-reperfusion injury.
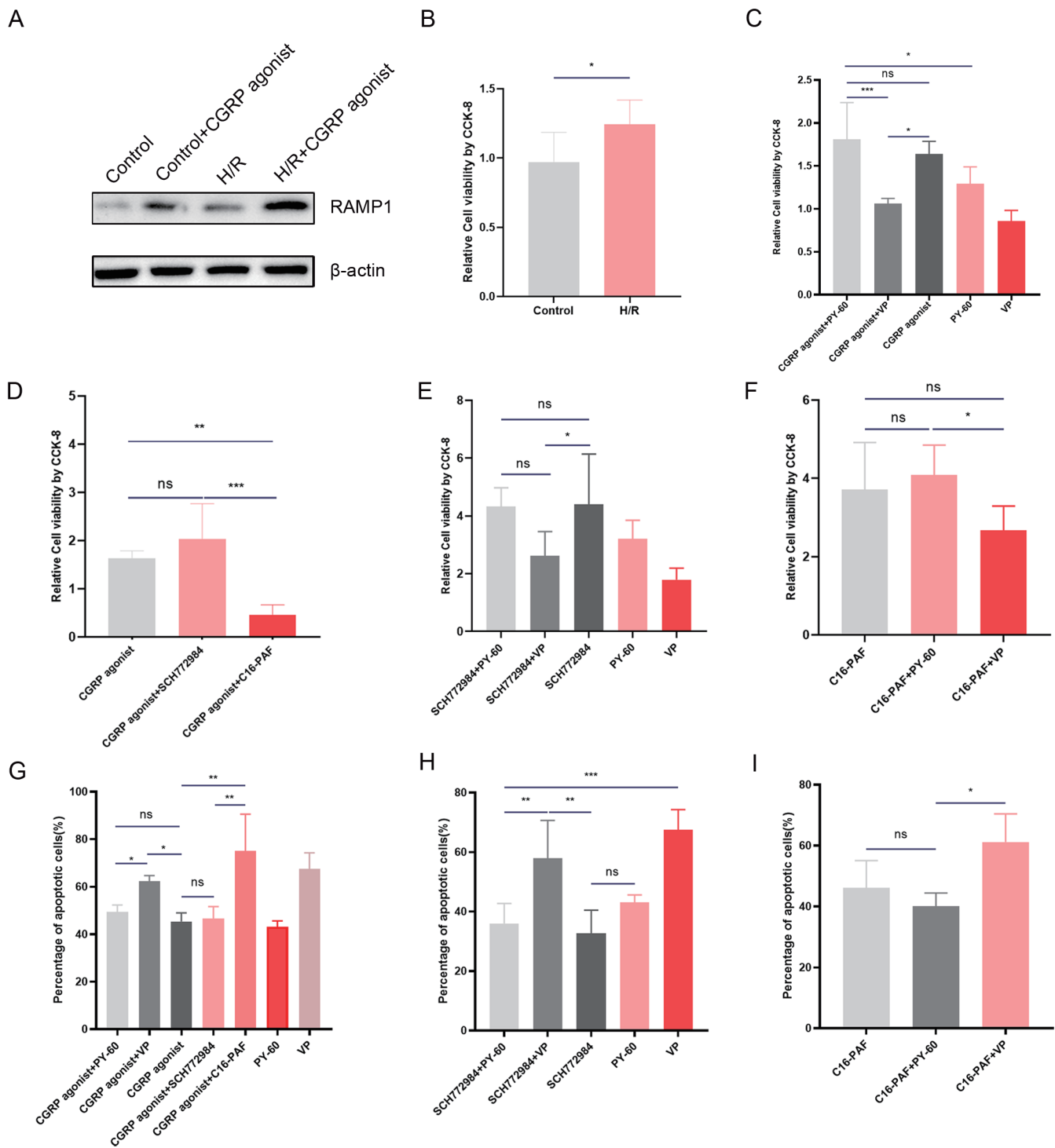
Fig. 7. Regulatory interplay among RAMP1, ERK, and YAP during HIRI. (A) Protein levels of RAMP1 in Control and H/R groups with and without CGRP agonist. (B) Relative cell activity was determined by CCK-8 assay of RAMP1 in the control and H/R groups using a CGRP agonist. (C) CCK-8 assay was performed using CGRP agonists, YAP inhibitors, and agonists in H/R. (D) CCK-8 assay was performed using a CGRP agonist combined with an ERK inhibitor or agonist in H/R. (E) CCK-8 experiments were performed using ERK inhibitors in combination with YAP inhibitors or agonists in H/R. (F) CCK-8 assays were performed using ERK agonists combined with a YAP inhibitor or agonist in H/R. (G) Statistical analysis of flow cytometry to detect the proportion of apoptosis in H/R with a CGRP agonist, YAP inhibitor and agonist, and ERK inhibitor and agonist. (H) Statistical data in H/R, ERK inhibitor combined with YAP inhibitor or agonist were used to detect the proportion of apoptosis by flow cytometry. (I) Statistical data in H/R using ERK agonists combined with YAP inhibitors or agonists to detect the proportion of apoptosis. CGRP agonist: Caltonin gene-related peptide (CGRP) II, rat TFA, ERK agonist (C16-PAF); ERK inhibitor (SCH772984); YAP agonist (PY-60); and YAP inhibitor (Verteporfin). The cells were treated with apoptosis pathway inhibitors and subjected to 6 h of reperfusion after hypoxia. All data are presented as the mean ± SD. *$p<0.05$, **$p<0.01$, ***$p<0.001$ using Student's two-tailed t-test. CCK-8, cell counting Kit-8; CGRP agonist, caltonin gene-related peptide agonist; HIRI, hepatic ischemia-reperfusion injury.

cell activity during H/R and C16-PAF + PY-60 increased this activity (Fig. 7E, F). These findings were corroborated by flow cytometry; the co-administration of the CGRP agonist with SCH772984 or PY-60 significantly reduced the proportion of apoptotic cells during H/R, whereas the co-administration of the CGRP agonist with C16-PAF or Verteporfin significantly increased this proportion (Fig. 7G, Supplementary Fig. 5A). Under H/R, SCH772984 + verteporfin and C16-PAF + Verteporfin substantially increased the proportion of apoptotic cells, whereas co-administration with PY-60 and C16-PAF + PY-60 significantly reduced this proportion (Fig. 7H, I, Supplementary Fig. 5B, C). These results strongly indicate that RAMP1 plays a role in the mitigation of hepatocyte injury by decreasing the phosphorylation of ERK1/2, which in turn leads to the reduction of YAP phosphorylation, during HIR.

Discussion

HIRI is a significant risk factor affecting survival after liver transplantation and contributing to donor shortages, and effective treatment strategies are urgently needed.[41,42] This study was the first in which the role of the RAMP1 gene in mice subjected to HIR was investigated, and its results provide insight contributing to the identification of a novel therapeutic target for HIRI. It revealed that RAMP1 expression is upregulated significantly during HIRI, that the RAMP1 gene protects against HIRI by reducing hepatocyte apoptosis, and that the mechanism potentially underlying this hepatoprotective effect is related to the phosphorylation of YAP and the ERK/MAPK pathway.

In mice, RAMP1 deficiency leads to increased macrophage and mast cell infiltration of colon tissue and the elevation of TNF-α and IL-1β levels, and RAMP1-KO exacerbates dextran sulfate sodium–induced colitis.[9] and increases inflammation, tissue edema, and pancreatic injury in the early stages of acute pancreatitis.[10] RAMP1 has also been found to regulate the Hippo/Yap pathway and to promote CGRP-induced osteogenic differentiation of BMSCs.[43] Its overexpression stimulates the proliferation of MSF through the Gαi3–PKA–CREB–YAP axis.[11] Furthermore, RAMP1 deficiency severely impairs organ mass recovery and hepatocyte proliferation after acute and chronic liver injury.[14] The protective effect of RAMP1 in different organs is supported by abundant evidence. Similarly, our recent studies have shown that RAMP1 plays a beneficial role under pathological conditions. H&E and TUNEL staining and liver function testing revealed aggravated liver tissue damage in RAMP1-KO mice relative to that in WT mice during IRI, but a minimal effect on RAMP1-KO liver tissue under physiological conditions, suggesting that RAMP1 helps to reduce the damage to liver structure and function during IRI. Given the critical role of RAMP1 in HIRI and its classification as a GPCR,[8] these findings suggest that RAMP1 could serve as a therapeutic target for future drug development, paving the way for further clinical applications.

HIRI is characterized by apoptosis, but the underlying mechanism remains unclear.[44] Several signal transduction pathways, including ERK/MAPK, have been found to play crucial roles in HIRI.[19] The inhibition of the ERK/MAPK pathway has a protective effect during HIRI. Carbon monoxide (CO), for instance, inhibits the expression of early pro-inflammatory and stress response genes and effectively improves HIRI by activating the CO–MEK/ERK1/2 signaling pathway.[45] Pretreatment with cafestol, a natural diterpene extract from coffee beans found mainly in unfiltered coffee, reduces ALT and AST levels, inhibits apoptosis, reduces the release of inflammatory mediators, and alleviates pathological liver damage, mainly by inhibiting ERK- and PPARγ-related path-

ways.[46] Melatonin regulates the TLR-mediated inflammatory response and improves I/R-induced liver damage by blunting JNK and ERK phosphorylation.[47] Cyclopamine pretreatment significantly reduces ERK phosphorylation and protects liver function after IRI.[48] ERK1/2 plays a crucial role in the regulation of upstream factors contributing to apoptotic events by activating downstream transcription factors, inducing the release of cytochrome C, down-regulation of Bcl-2, and up-regulation of Bax. It also promotes apoptosis by activating and upregulating the expression of Caspases 3, 8, and 9.[49,50] In this study, the subjection of RAMP1-deficient mice and cells to HIR significantly increased ERK activation and phosphorylation; treatment with SCH772984 inhibited ERK signaling, partially reversed the elevation of ERK phosphorylation, and reduced the rate of apoptosis. In addition, RAMP1-deficient mice exhibited significantly increased expression of pro-apoptotic proteins and decreased expression of anti-apoptotic genes compared with WT mice. These findings strongly suggest that RAMP1 plays a key role in the regulation of apoptosis in hepatocytes through the ERK/MAPK pathway.

YAP has been identified as a crucial component of the mammalian Hippo signaling pathway,[51,52] and recent research has indicated it's involvement in the regulation of apoptosis.[53–56] For instance, YAP has been shown to play a role in glucose metabolism by promoting the expression of GLUT3, researchers have suggested that glucose starvation activates the Hippo–YAP signaling pathway, and YAP regulates apoptosis by controlling glucose uptake.[57] Additionally, when normal blood cells experience DNA damage–related stress, the tyrosine kinase C-ABL translocates to the nucleus and phosphorylates YAP at Y357 on tyrosine residues.[58] This phosphorylated YAP binds to p73 and promotes the transcription of pro-apoptotic genes such as p53AIPI,[55] Bax,[53] and PUMA.[54] YAP interacts with TEAD transcription factors in the nucleus, leading to the upregulation of anti-apoptotic genes.[59–61] Our findings suggest that the anti-apoptotic effect of RAMP1 in hepatocytes is related to the regulation of the ERK/MAPK pathway and the function and phosphorylation of YAP. RAMP1 contributes to the reduction of hepatocyte injury by diminishing the phosphorylation of ERK, leading to a decrease in YAP phosphorylation.

RAMP1 is a critical protein in CGRP receptor signaling, and RAMP1-KO has been demonstrated to impede CGRP function.[13,14] Thus, we think that the mechanism underlying RAMP1's regulation of HIRI involves the activation of CGRP, which, in turn, directly stimulates an increase in cAMP signaling. During I/R, the phosphorylation of ERK and YAP increases, leading to liver cell apoptosis and damage. CGRP-induced cAMP signaling may directly mitigate cell damage by inhibiting the phosphorylation of ERK and YAP. The findings of this study provide valuable insight into the biological role of RAMP1 and the mechanisms underlying RAMP1 damage in HIRI. RAMP1-targeted interventions may provide strategies for reducing IRI in various settings, including partial hepatectomy and liver transplantation.

Conflict of interest

The authors have no conflict of interests related to this publication.

Author contributions

HL, CJ, YT, and ZY conceived and designed the study. YT and ZY performed the experiments. XL and YS analyzed the data. SZ, CQ, QZ and BF contributed reagents and material tools. YT and CJ drafted the manuscript.

Ethical statement

All experimental procedures were approved by the Animal Care and Use Committee of the Ruiye Animal Model Center and were commissioned by the Third Affiliated Hospital of Sun Yat-sen University. Number of experimental animal ethical inspection tab: RYEth-20230603255.

Data sharing statement

The datasets generated during and/or analyzed during the study are available from the corresponding author upon reasonable request.

References

[1] Peralta C, Jimenez-Castro MB, Gracia-Sancho J. Hepatic ischemia and reperfusion injury: effects on the liver sinusoidal milieu. J Hepatol 2013;59(5):1094–1106. doi:10.1016/j.jhep.2013.06.017, PMID:23811302.

[2] Tanaka S, Hikita H, Tatsumi T, Sakamori R, Nozaki Y, Sakane S, *et al*. Rubicon inhibits autophagy and accelerates hepatocyte apoptosis and lipid accumulation in nonalcoholic fatty liver disease in mice. Hepatology 2016;64(6):1994–2014. doi:10.1002/hep.28820, PMID:27637015.

[3] Changizi Z, Kajbaf F, Moslehi A. An Overview of the Role of Peroxisome Proliferator-activated Receptors in Liver Diseases. J Clin Transl Hepatol 2023;11(7):1542–1552. doi:10.14218/JCTH.2023.00334, PMID:38161499.

[4] Cadenas S. ROS and redox signaling in myocardial ischemia-reperfusion injury and cardioprotection. Free Radic Biol Med 2018;117:76–89. doi:10.1016/j.freeradbiomed.2018.01.024, PMID:29373843.

[5] Xue Q, Pei H, Liu Q, Zhao M, Sun J, Gao E, *et al*. MICU1 protects against myocardial ischemia/reperfusion injury and its control by the importer receptor Tom70. Cell Death Dis 2017;8(7):e2923. doi:10.1038/cddis.2017.280, PMID:28703803.

[6] Toldo S, Mauro AG, Cutter Z, Abbate A. Inflammasome, pyroptosis, and cytokines in myocardial ischemia-reperfusion injury. Am J Physiol Heart Circ Physiol 2018;315(6):H1553–H1568. doi:10.1152/ajpheart.00158.2018, PMID:30168729.

[7] Praetner M, Zuchtriegel G, Holzer M, Uhl B, Schaubächer J, Mittmann L, *et al*. Plasminogen Activator Inhibitor-1 Promotes Neutrophil Infiltration and Tissue Injury on Ischemia-Reperfusion. Arterioscler Thromb Vasc Biol 2018;38(4):829–842. doi:10.1161/ATVBAHA.117.309760, PMID:29371242.

[8] Blixt FW, Radziwon-Balicka A, Edvinsson L, Warfvinge K. Distribution of CGRP and its receptor components CLR and RAMP1 in the rat retina. Exp Eye Res 2017;161:124–131. doi:10.1016/j.exer.2017.06.002, PMID:28603014.

[9] Kawashima-Takeda N, Ito Y, Nishizawa N, Kawashima R, Tanaka K, Tsujikawa K, *et al*. RAMP1 suppresses mucosal injury from dextran sodium sulfate-induced colitis in mice. J Gastroenterol Hepatol 2017;32(4):809–818. doi:10.1111/jgh.13505, PMID:27513455.

[10] Jochheim LS, Odysseos G, Hidalgo-Sastre A, Zhong S, Staufer LM, Kroiss M, *et al*. The neuropeptide receptor subunit RAMP1 constrains the innate immune response during acute pancreatitis in mice. Pancreatology 2019;19(4):541–547. doi:10.1016/j.pan.2019.05.455, PMID:31109903.

[11] Yin S, Song R, Ma J, Liu C, Wu Z, Cao G, *et al*. Receptor activity-modifying protein 1 regulates mouse skin fibroblast proliferation via the Galphai3-PKA-CREB-YAP axis. Cell Commun Signal 2022;20(1):52. doi:10.1186/s12964-022-00852-0, PMID:35413847.

[12] Mishima T, Ito Y, Nishizawa N, Amano H, Tsujikawa K, Miyaji K, *et al*. RAMP1 signaling improves lymphedema and promotes lymphangiogenesis in mice. J Surg Res 2017;219:50–60. doi:10.1016/j.jss.2017.05.124, PMID:29078910.

[13] Barwell J, Wootten D, Simms J, Hay DL, Poyner DR. RAMPs and CGRP receptors. Adv Exp Med Biol 2012;744:13–24. doi:10.1007/978-1-4614-2364-5_2, PMID:22434104.

[14] Laschinger M, Wang Y, Holzmann G, Wang B, Stoss C, Lu M, *et al*. The CGRP receptor component RAMP1 links sensory innervation with YAP activity in the regenerating liver. FASEB J 2020;34(6):8125–8138. doi:10.1096/fj.201903200R, PMID:32329113.

[15] Suekane A, Ichikawa T, Saito Y, Nakahata S, Morishita K. The CGRP Receptor Antagonist MK0974 Induces EVI1(high) AML Cell Apoptosis by Disrupting ERK Signaling. Anticancer Res 2022;42(10):4743–4752. doi:10.21873/anticanres.15979, PMID:36191988.

[16] Sun Y, Liu WZ, Liu T, Feng X, Yang N, Zhou HF. Signaling pathway of MAPK/ERK in cell proliferation, differentiation, migration, senescence and apoptosis. J Recept Signal Transduct Res 2015;35(6):600–604. doi:10.3109/10799893.2015.1030412, PMID:26096166.

[17] Hou X, Huang M, Zeng X, Zhang Y, Sun A, Wu Q, *et al*. The Role of TRPC6 in Renal Ischemia/Reperfusion and Cellular Hypoxia/Reoxygenation Injuries. Front Mol Biosci 2021;8:698975. doi:10.3389/fmolb.2021.698975, PMID:34307458.

[18] Fawzy MA, Maher SA, Bakkar SM, El-Rehany MA, Fathy M. Pantoprazole Attenuates MAPK (ERK1/2, JNK, p38)-NF-kappaB and Apoptosis Signaling Pathways after Renal Ischemia/Reperfusion Injury in Rats. Int J Mol Sci 2021;22(19):669. doi:10.3390/ijms221910669, PMID:34639009.

[19] Yu B, Zhang Y, Wang T, Guo J, Kong C, Chen Z, *et al*. MAPK Signaling Pathways in Hepatic Ischemia/Reperfusion Injury. J Inflamm Res 2023;16:1405–1418. doi:10.2147/JIR.S396604, PMID:37012971.

[20] Yan ZZ, Huang YP, Wang X, Wang HP, Ren F, Tian RF, *et al*. Integrated Omics Reveals Tollip as an Regulator and Therapeutic Target for Hepatic Ischemia-Reperfusion Injury in Mice. Hepatology 2019;70(5):1750–1769. doi:10.1002/hep.30705, PMID:31077413.

[21] Zhou J, Hu M, He M, Wang X, Sun D, Huang Y, *et al*. TNFAIP3 Interacting Protein 3 Is an Activator of Hippo-YAP Signaling Protecting Against Hepatic Ischemia/Reperfusion Injury. Hepatology 2021;74(4):2133–2153. doi:10.1002/hep.32015, PMID:34133792.

[22] Qin JJ, Mao W, Wang X, Sun P, Cheng D, Tian S, *et al*. Caspase recruitment domain 6 protects against hepatic ischemia/reperfusion injury by suppressing ASK1. J Hepatol 2018;69(5):1110–1122. doi:10.1016/j.jhep.2018.06.014, PMID:29958938.

[23] Suzuki S, Toledo-Pereyra LH, Rodriguez FJ, Cejalvo D. Neutrophil infiltration as an important factor in liver ischemia and reperfusion injury. Modulating effects of FK506 and cyclosporine. Transplantation 1993;55(6):1265–1272. doi:10.1097/00007890-199306000-00011, PMID:7685932.

[24] Mederacke I, Dapito DH, Affò S, Uchinami H, Schwabe RF. High-yield and high-purity isolation of hepatic stellate cells from normal and fibrotic mouse livers. Nat Protoc 2015;10(2):305–315. doi:10.1038/nprot.2015.017, PMID:25612230.

[25] Kastan N, Gnedeva K, Alisch T, Petelski AA, Huggins DJ, Chiaravalli J, *et al*. Small-molecule inhibition of Lats kinases promotes Yap-dependent proliferation in postmitotic mammalian tissues. Nat Commun 2021;12(1):3100. doi:10.1038/s41467-021-23395-3, PMID:34035288.

[26] Shalhout SZ, Yang PY, Grzelak EM, Nutsch K, Shao S, Zambaldo C, *et al*. YAP-dependent proliferation by a small molecule targeting annexin A2. Nat Chem Biol 2021;17(7):767–775. doi:10.1038/s41589-021-00755-0, PMID:33723431.

[27] Bhagwat SV, McMillen WT, Cai S, Zhao B, Whitesell M, Kindler L, *et al*. Abstract 4973: Discovery of LY3214996, a selective and novel ERK1/2 inhibitor with potent antitumor activities in cancer models with MAPK pathway alterations. Cancer Res 2017;77(13_Supplement):4973. doi:10.1158/1538-7445.Am2017-4973.

[28] Morris EJ, Jha S, Restaino CR, Dayananth P, Zhu H, Cooper A, *et al*. Discovery of a novel ERK inhibitor with activity in models of acquired resistance to BRAF and MEK inhibitors. Cancer Discov 2013;3(7):742–750. doi:10.1158/2159-8290.CD-13-0070, PMID:23614898.

[29] Morris EJ, Jha S, Restaino CR, Dayananth P, Zhu H, Cooper A, *et al*. Discovery of a Novel ERK Inhibitor with Activity in Models of Acquired Resistance to BRAF and MEK Inhibitors. Cancer Discov 2013;3(7):742–750. doi:10.1158/2159-8290.CD-13-0070, PMID:23614898.

[30] Ryan SD, Harris CS, Carswell CL, Baenziger JE, Bennett SAL. Heterogeneity in the sn-1 carbon chain of platelet-activating factor glycerophospholipids determines pro- or anti-apoptotic signaling in primary neurons. J Lipid Res 2008;49(10):2250–2258. doi:10.1194/jlr.M800263-JLR200, PMID:18550892.

[31] Bögershausen N, Tsai IC, Pohl E, Kiper PÖS, Beleggia F, Percin EF, *et al*. RAP1-mediated MEK/ERK pathway defects in Kabuki syndrome. J Clin Invest 2015;125(9):3585–3599. doi:10.1172/JCI80102, PMID:26280580.

[32] Yokota T, Omachi K, Suico MA, Kamura M, Kojima H, Fukuda R, *et al*. STAT3 inhibition attenuates the progressive phenotypes of Alport syndrome mouse model. Nephrol Dial Transplant 2018;33(2):214–223. doi:10.1093/ndt/gfx246, PMID:28992339.

[33] Xing Y, Lin NU, Maurer MA, Chen H, Mahvash A, Sahin A, *et al*. Phase II trial of AKT inhibitor MK-2206 in patients with advanced breast cancer who have tumors with PIK3CA or AKT mutations, and/or PTEN loss/PTEN mutation. Breast Cancer Res 2019;21(1):78. doi:10.1186/s13058-019-1154-8, PMID:31277699.

[34] Liu X, Nie L, Zhang Y, Yan Y, Wang C, Colic M, *et al*. Actin cytoskeleton vulnerability to disulfide stress mediates disulfidptosis. Nat Cell Biol 2023;25(3):404–414. doi:10.1038/s41556-023-01091-2, PMID:36747082.

[35] van den Berg E, Bal SM, Kuipers MT, Matute-Bello G, Lutter R, Bos AP,

et al. The caspase inhibitor zVAD increases lung inflammation in pneu-movirus infection in mice. Physiol Rep 2015;3(3):e12332. doi:10.14814/phy2.12332, PMID:25780096.

[36] Wisskirchen FM, Marshall I. CGRP2 receptor in the internal anal sphincter of the rat: implications for CGRP receptor classification. Br J Pharmacol 2000;130(2):464–470. doi:10.1038/sj.bjp.0703315, PMID:10807687.

[37] Wang X, Ji L, Wang J, Liu C. Matrix stiffness regulates osteoclast fate through integrin-dependent mechanotransduction. Bioact Mater 2023;27:138–153. doi:10.1016/j.bioactmat.2023.03.014, PMID:37064801.

[38] Wang Y, Gao J, Zhang D, Zhang J, Ma J, Jiang H. New insights into the antifibrotic effects of sorafenib on hepatic stellate cells and liver fibro-sis. J Hepatol 2010;53(1):132–144. doi:10.1016/j.jhep.2010.02.027, PMID:20447716.

[39] Xu D, Liu L, Zhao Y, Yang L, Cheng J, Hua R, *et al*. Melatonin protects mouse testes from palmitic acid-induced lipotoxicity by attenuating oxida-tive stress and DNA damage in a SIRT1-dependent manner. J Pineal Res 2020;69(4):e12690. doi:10.1111/jpi.12690, PMID:32761924.

[40] Zhao Z, Li F, Ning J, Peng R, Shang J, Liu H, *et al*. Novel compound FLZ al-leviates rotenone-induced PD mouse model by suppressing TLR4/MyD88/NF-κB pathway through microbiota–gut–brain axis. Acta Pharm Sin B 2021;11(9):2859–2879. doi:10.1016/j.apsb.2021.03.020, PMID:34589401.

[41] Eltzschig HK, Eckle T. Ischemia and reperfusion—from mechanism to translation. Nat Med 2011;17(11):1391–1401. doi:10.1038/nm.2507, PMID:22064429.

[42] Liu H, Man K. New Insights in Mechanisms and Therapeutics for Short- and Long-Term Impacts of Hepatic Ischemia Reperfusion Injury Post Liver Trans-plantation. Int J Mol Sci 2021;22(15):8210. doi:10.3390/ijms22158210, PMID:34360975.

[43] Zhang Q, Guo Y, Yu H, Tang Y, Yuan Y, Jiang Y, *et al*. Receptor activity-mod-ifying protein 1 regulates the phenotypic expression of BMSCs via the Hip-po/Yap pathway. J Cell Physiol 2019;234(8):13969–13976. doi:10.1002/jcp.28082, PMID:30618207.

[44] Zhai M, Li B, Duan W, Jing L, Zhang B, Zhang M, *et al*. Melatonin ameliorates myocardial ischemia reperfusion injury through SIRT3-dependent regula-tion of oxidative stress and apoptosis. J Pineal Res 2017;63(2):e12419. doi:10.1111/jpi.12419, PMID:28500761.

[45] Kaizu T, Ikeda A, Nakao A, Tsung A, Toyokawa H, Ueki S, *et al*. Protection of transplant-induced hepatic ischemia/reperfusion injury with carbon mon-oxide via MEK/ERK1/2 pathway downregulation. Am J Physiol Gastroin-test Liver Physiol 2008;294(1):G236–244. doi:10.1152/ajpgi.00144.2007, PMID:18006605.

[46] Ji J, Wu L, Feng J, Mo W, Wu J, Yu Q, *et al*. Cafestol preconditioning at-tenuates apoptosis and autophagy during hepatic ischemia-reperfusion injury by inhibiting ERK/PPARgamma pathway. Int Immunopharmacol 2020;84:106529. doi:10.1016/j.intimp.2020.106529, PMID:32344356.

[47] Kang JW, Koh EJ, Lee SM. Melatonin protects liver against ischemia and rep-erfusion injury through inhibition of toll-like receptor signaling pathway. J Pineal Res 2011;50(4):403–411. doi:10.1111/j.1600-079X.2011.00858.x, PMID:21355876.

[48] Pratap A, Panakanti R, Yang N, Eason JD, Mahato RI. Inhibition of endog-enous hedgehog signaling protects against acute liver injury after ischemia reperfusion. Pharm Res 2010;27(11):2492–2504. doi:10.1007/s11095-010-0246-z, PMID:20737284.

[49] Lavoie H, Gagnon J, Therrien M. ERK signalling: a master regulator of cell behaviour, life and fate. Nat Rev Mol Cell Biol 2020;21(10):607–632. doi:10.1038/s41580-020-0255-7, PMID:32576977.

[50] Jaiswal BS, Durinck S, Stawiski EW, Yin J, Wang W, Lin E, *et al*. ERK Muta-tions and Amplification Confer Resistance to ERK-Inhibitor Therapy. Clin Cancer Res 2018;24(16):4044–4055. doi:10.1158/1078-0432.CCR-17-3674, PMID:29760222.

[51] Wang J, Liu S, Heallen T, Martin JF. The Hippo pathway in the heart: piv-otal roles in development, disease, and regeneration. Nat Rev Cardiol 2018;15(11):672–684. doi:10.1038/s41569-018-0063-3, PMID:30111784.

[52] Hilman D, Gat U. The evolutionary history of YAP and the hippo/YAP path-way. Mol Biol Evol 2011;28(8):2403–2417. doi:10.1093/molbev/msr065, PMID:21415026.

[53] Strano S, Monti O, Pediconi N, Baccarini A, Fontemaggi G, Lapi E, *et al*. The transcriptional coactivator Yes-associated protein drives p73 gene-target specificity in response to DNA Damage. Mol Cell 2005;18(4):447–459. doi:10.1016/j.molcel.2005.04.008, PMID:15893728.

[54] Matallanas D, Romano D, Yee K, Meissl K, Kucerova L, Piazzolla D, *et al*. RASSF1A elicits apoptosis through an MST2 pathway directing proapoptotic transcription by the p73 tumor suppressor protein. Mol Cell 2007;27(6):962–975. doi:10.1016/j.molcel.2007.08.008, PMID:17889669.

[55] Lapi E, Di Agostino S, Donzelli S, Gal H, Domany E, Rechavi G, *et al*. PML, YAP, and p73 are components of a proapoptotic autoregulatory feedback loop. Mol Cell 2008;32(6):803–814. doi:10.1016/j.molcel.2008.11.019, PMID:19111660.

[56] Zhang X, Abdelrahman A, Vollmar B, Zechner D. The Ambivalent Func-tion of YAP in Apoptosis and Cancer. Int J Mol Sci 2018;19(12):3770. doi:10.3390/ijms19123770, PMID:30486435.

[57] Wang W, Xiao ZD, Li X, Aziz KE, Gan B, Johnson RL, *et al*. AMPK modu-lates Hippo pathway activity to regulate energy homeostasis. Nat Cell Biol 2015;17(4):490–499. doi:10.1038/ncb3113, PMID:25751139.

[58] Levy D, Adamovich Y, Reuven N, Shaul Y. Yap1 phosphorylation by c-Abl is a critical step in selective activation of proapoptotic genes in response to DNA damage. Mol Cell 2008;29(3):350–361. doi:10.1016/j.mol-cel.2007.12.022, PMID:18280240.

[59] Li W, Cao Y, Xu J, Wang Y, Li W, Wang Q, *et al*. YAP transcriptionally regu-lates COX-2 expression and GCCSysm-4 (G-4), a dual YAP/COX-2 inhibi-tor, overcomes drug resistance in colorectal cancer. J Exp Clin Cancer Res 2017;36(1):144. doi:10.1186/s13046-017-0612-3, PMID:29037225.

[60] Lin C, Xu X. YAP1-TEAD1-Glut1 axis dictates the oncogenic phenotypes of breast cancer cells by modulating glycolysis. Biomed Pharmacother 2017;95:789–794. doi:10.1016/j.biopha.2017.08.091, PMID:28892790.

[61] Ma K, Xu Q, Wang S, Zhang W, Liu M, Liang S, *et al*. Nuclear accumu-lation of Yes-Associated Protein (YAP) maintains the survival of doxo-rubicin-induced senescent cells by promoting survivin expression. Can-cer Lett 2016;375(1):84–91. doi:10.1016/j.canlet.2016.02.045, PMID:26944315.